THE ASTROPHYSICAL JOURNAL, 295:183–194, 1985 August 1

THE DETECTION OF ROTATIONALLY EXCITED OH EMISSION TOWARD THE PROBABLE YOUNG PLANETARY NEBULA Vy 2-2

P. R. JEWELL,[1] M. S. SCHENEWERK, AND L. E. SNYDER
Department of Astronomy, University of Illinois, Urbana
Received 1984 November 20; accepted 1985 February 13

ABSTRACT

A search for 4.7 and 6.0 GHz rotationally excited OH emission in OH/Miras, OH/IR stars, Herbig-Haro objects, Herbig Ae and Be stars, and compact planetary nebulae has been performed. Many of the objects were surveyed in all seven of the lambda doublet hyperfine transitions in the $^2\Pi_{3/2}$, $J = 5/2$ and $^2\Pi_{1/2}$, $J = 1/2$ rotational states. In general, this is the most comprehensive and sensitive search for circumstellar rotationally excited OH yet performed. Only one new detection was made, but that was of 6035 MHz emission from the interesting object Vy 2-2. This object is a probable compact planetary nebula surrounded by a fossil molecular envelope from the progenitor red giant. The object was previously known to have a 1612 MHz ground-state OH maser.

A complete summary of all observations is given. We discuss the excitation conditions and a number of pumping schemes that could explain the Vy 2-2 masers and the negative results for excited-state OH masers in the other sources. The morphology of the Vy 2-2 envelope as indicated by the velocity structure of the 6035 MHz emissions is also discussed.

Subject headings: interstellar: molecules — masers — nebulae: individual — nebulae: planetary

I. INTRODUCTION

Much of what is known about the circumstellar envelopes of evolved, oxygen-rich giant stars has been provided by ground-state OH maser studies. Such basic characteristics as envelope expansion velocity, diameter, and structure; the position, distance, and systemic velocity of the source; and the mass-loss rate of the central star are all derivable—often exclusively—from OH maser observations. Conversely, important parameters such as the envelope abundances and excitation usually are not easily derivable from OH maser observations. These quantities are most often obtained through detailed computer models involving numerous variables that must be fitted to comparatively few observables. One way to constrain the models of OH abundance and excitation is to observe transitions in the excited rotational states in addition to the well-known ground-state transitions.

Although previous searches for rotationally excited OH have been mostly negative (e.g., Thacker, Wilson, and Barrett 1970; Zuckerman *et al.* 1972; Baudry 1974; Rickard, Zuckerman, and Palmer 1975; Claussen and Fix 1981), two recent developments suggested that a new search might be fruitful. First, a significant improvement in receiver sensitivity, particularly at 6 GHz, has been achieved. Second, numerous new candidate objects have been identified, including entire categories of objects such as OH/IR stars and compact planetary nebulae. We report in this paper the results of extensive searches for circumstellar rotationally excited OH emission in the $^2\Pi_{3/2}$, $J = 5/2$ transitions near 6.0 GHz and the $^2\Pi_{1/2} = J = 1/2$ transitions near 4.7 GHz.

A primary result of our searches was the detection of the 6035 MHz OH line toward the compact nebula Vyssotsky 2-2. This source is apparently a member of the emerging class of evolved stellar objects in transition from red giant to planetary nebula. It is classified as a compact planetary nebula (e.g., Perek and Kohoutek 1967) with moderate-excitation optical emission lines (Kaler 1976) and is well known as a thermal radio continuum source (Marsh 1975; Purton *et al.* 1982). A few years ago Vy 2-2 was also discovered to be the probable host of a ground-state OH maser at 1612 MHz (Davis, Seaquist, and Purton 1979, hereafter DSP). The association has been recently confirmed by aperture synthesis mapping (Seaquist and Davis 1983). Since the object has both an ionized zone and a neutral, molecular cloud, DSP suggested that it was a very young planetary nebula still enveloped by the neutral circumstellar shell of the progenitor red giant. If this interpretation is correct, the object assumes considerable importance in the study of planetary nebula formation. Only a few objects have been proposed to be in transition from red giant to planetary nebula (e.g., GL 2688, IRC +10420, GL 618). Even fewer bona fide planetary nebulae are suggested to have fossil red giant molecular envelopes still intact (e.g., NGC 7027). Among this latter group, only Vy 2-2 is apparently oxygen rich, as is evidenced by its OH maser.

The 6035 MHz OH line from Vy 2-2 arises from an energy level ~120 K above the ground state. The maser thus samples an excitation regime that is significantly different from that of the ground state. In this paper we discuss the information provided by the excited-state OH line on OH maser pumping, envelope excitation, velocity structure, and spatial structure of Vy 2-2.

We additionally discuss our searches for rotationally excited OH toward long-period variable stars, planetary nebulae, Herbig-Haro objects, and Herbig Ae-Be stars. For comparison purposes, we observed several previously known sources of rotationally excited OH in H II/molecular cloud regions. The results of these observations are presented in tabular form. Earlier reports of rotationally excited OH in the evolved circumstellar objects NML Cyg and AU Gem are discussed in light of the present observations.

[1] Currently at the National Radio Astronomy Observatory, Tucson.

TABLE 1

OH TRANSITIONS AND OBSERVING PARAMETERS

		T_{sys}(K)			
TRANSITION[a]	RELATIVE INTENSITY[b]	1980 Sep	1981 Apr	1981 Aug	1982 May
$^2\Pi_{1/2}, J = 1/2$:					
$F = 0 \rightarrow 1$, 4660.242 MHz	1.5	77	...	70	58
$F = 1 \rightarrow 1$, 4750.656 MHz	2	78	...	48	61
$F = 1 \rightarrow 0$, 4765.562 MHz	1	79	...	46	52
$^2\Pi_{3/2}, J = 5/2$:					
$F = 2 \rightarrow 3$, 6016.746 MHz	1	...	58	38	37
$F = 2 \rightarrow 2$, 6030.747 MHz	14	...	60	41	39
$F = 3 \rightarrow 3$, 6035.092 MHz	20	...	58	41	39
$F = 3 \rightarrow 2$, 6049.084 MHz	1	...	58	...	45

[a] Meerts and Dymanus 1975.
[b] Radford 1968.

II. INSTRUMENTATION

The observations were made with the NRAO[2] 43 m telescope in Green Bank, West Virginia during four observing sessions: 1980 September 26–30, 1981 April 18–23, 1981 August 28–31, and 1982 May 7–13. The transition frequencies, relative line strengths under equilibrium conditions, and characteristic system noise temperatures are listed in Table 1. In 1980 September, the front-end receiver was a cooled, parametric amplifier. In 1981 April, the excellent 4.7–7.2 GHz maser upconverter developed by C. Brockway was used. This system, with added improvements, was used again in 1981 August and 1982 May. The spectrometer for all four observing sessions was the 1024 channel Model IV autocorrelator. The instantaneous bandwidth of the front-end receiver was usually broad enough to include two or more transition frequencies of a particular OH lambda doublet. When possible, the autocorrelator was split into halves, and two transitions were observed simultaneously. Typical bandwidths used were 1.25 or 2.50 MHz.

During the 1980 September observations, we used a position switching observing mode with the reference position offset 30′ in right ascension from the source position. During the latter three sessions, frequency switching was used with the reference band usually offset by one full bandwidth. In a few instances, overlapped frequency switching, in which the signal frequency appears in both signal and reference, was used. Temperature calibration was obtained with a standard noise injection procedure. Flux density calibration was achieved by observing the calibration source 3C 286. Using the scale of Baars *et al.* (1977) which predicts a flux from 3C 286 of 7.54 Jy at 4750 MHz and 6.48 Jy at 6030 MHz, we obtained aperture efficiencies of 53% ($S/T_A = 3.66$ Jy K^{-1}) at 4750 MHz and 52% ($S/T_A = 3.68$ Jy K^{-1}) at 6030 MHz. Telescope beamwidths (FWHM) were 6$'$.0 at 4.7 GHz and 4$'$.8 at 6.0 GHz. All observations were made with a single, linearly polarized feed with a position angle of 0° in 1980 September and 157°.5 for the other sessions.

III. OBSERVATIONS

The sources chosen for this survey encompass a variety of physical conditions and states of evolution. Table 2 provides a list of the sources, their 1950 coordinates and the literature references for those coordinates, the assumed center velocities, and the type of source. For long-period variables with available phase information, we have listed the phase at each observing epoch. Most Mira phases were calculated from the data of the American Association of Variable Star Observers (AAVSO). The phase of IRC +10011 was extrapolated from the OH maser monitoring observations described by Jewell, Webber, and Snyder (1980), and the phases of OH 127.8−0.0, VY CMa, WX Ser, OH 17.7−2.0, and NML Cyg were computed from the OH monitoring data of Herman (1983).

The energy level diagram in Figure 1 shows the transitions of the first two rotationally excited OH states together with the familiar ground state. Table 3 summarizes all the observations made, and Table 4 provides additional information on detected lines. The entries in these tables are explained in the table footnotes. The radial velocity search range listed in Tables 3 and 4 is the range of the final, displayed spectrum. The effective range is somewhat larger than that for observations made in the frequency switching mode, as emission lines appearing in the reference band would appear as absorption signals in the final spectrum. This may be of importance for the 1982 May observations of planetary nebulae and other objects with uncertain center velocities. Our usual observing mode placed the reference band higher in frequency (lower in velocity) by one bandwidth. The length of a typical search observation was about 1 hr, although some longer observations were made.

The 6035 MHz emission from Vy 2-2 was observed in both 1981 August and 1982 May and was the only new detection of this study (Fig. 2). We could not confirm the presence of rotationally excited OH masers in either NML Cyg or AU Gem, the only other evolved stellar objects reported to have such masers. Zuckerman *et al.* (1972) reported a line with a peak T_A of $\sim$0.8 K from NML Cyg, an M supergiant. We would have easily detected a line of this strength during either of the two sessions in which we searched for it. Whether this result indicates that the 6035 MHz emission from NML Cyg is episodic or that the line reported by Zuckerman *et al.* (1972) was spurious cannot be determined from the two data sets alone. Claussen and Fix (1981), observing with the Arecibo telescope, have reported a 4750 MHz line with a peak flux density of 0.10 Jy from the Mira variable AU Gem. We integrated to an rms noise level of 0.07 Jy at 4750 MHz toward AU Gem and saw no evidence for a line.. The feature reported by Claussen and Fix (1981) would be only $\sim$1.5 σ in our spectrum and, quite possibly, could be obscured by the noise. The present result suggests that AU Gem should be reobserved, however.

[2] The National Radio Astronomy Observatory is operated by Associated Universities, Inc., under contract with the National Science Foundation.

TABLE 2

SOURCES SEARCHED FOR ROTATIONALLY EXCITED OH EMISSION

Source	α(1950)	δ(1950)	V_{LSR} (km s^{-1})	Type[a]	Position Reference	LPV Phase[c] 1980 Sep 28	1981 Apr 21	1981 Aug 29
LkHα 198	00h08m43s.6	+58°33′08″	+30.0	AeBe	1	...	...	...
IRC +10011	01 03 48.1	+12 19 51	+9.0	OH/IR	2	0.17	0.49	0.66
OH 127.8−0.0	01 30 27.6	+62 11 31	−55.0	OH/IR	2	n.o.	0.47	n.o.
W3(OH)	02 23 16.8	+61 38 53	−44.5	MC/H II	3	...	...	...
IK Tau	03 50 46.0	+11 15 42	+33.0	OH/IR	4	n.o.	~0.2	n.o.
IRC +50137	05 07 19.7	+52 48 54	+5.0	OH/IR	2	...	...	...
HK Ori	05 28 41.8	+12 07 22	+11.0	AeBe	5	...	...	...
Orion A	05 32 46.9	−05 24 18	+7.0	MC/H II	6	...	...	...
M78	05 43 35.1	−00 11 02	0.0	HH	7	...	...	...
OH 205.1−14.1	05 44 33.0	+00 20 30	0.0	T Tau?	8	...	...	...
U Ori	05 52 51.0	+20 10 06	−39.0	OH/Mira	9	n.o.	0.54	n.o.
HD 250550	05 59 05.5	+16 31 10	+10.0	AeBe	5	...	...	...
HD 44179	06 17 37.0	−10 36 52	+27.0	?	9	...	...	...
VY CMa	07 20 54.7	−25 40 12	+21.0	OH/SG	2	~0.4	~0.6	~0.7
OH 231.8+4.2	07 39 58.9	−14 35 43	+30.0	BPN	10	...	...	...
AU Gem	07 42 17.2	+30 56 00	+5.0	OH/Mira	11	...	...	...
R Leo	09 44 52.0	+11 39 42	+1.0	OH/Mira	9	0.13	0.77	0.19
W Hya	13 46 12.2	−28 07 07	+40.0	OH/Mira	9	~0.9	~0.4	~0.8
S CrB	15 19 21.5	+31 32 47	+1.0	OH/Mira	9	n.o.	0.28	n.o.
WX Ser	15 25 32.0	+19 44 13	+5.8	OH/Mira	2	n.o.	0.88	n.o.
U Her	16 23 34.9	+19 00 18	−13.5	OH/Mira	9	n.o.	0.31	n.o.
M2−9	17 02 52.7	−10 04 26	+82.0	PN	12	...	...	...
NGC 6334N	17 17 32.1	−35 44 15	−10.0	MC/H II	6	...	...	...
M3−38	17 17 54.2	−29 00 03	0.0	PN	13	...	...	...
M1−26	17 42 45.0	−30 10 52	+5.0	PN	12	...	...	...
Sgr B2	17 44 11.0	−28 22 30	+60.0	MC/H II	14	...	...	...
VX Sgr	18 05 03.2	−22 14 06	+6.0	OH/SG	15	...	...	...
SwSt 1	18 12 58.6	−30 53 13	+0.0	PN	12	...	...	...
M17	18 17 29.0	−16 13 42	+21.5	MC/H II	14	...	...	...
IRC −10414	18 20 28.0	−13 44 06	+20.0	OH/IR	4	...	...	...
M3−27	18 25 31.6	+14 27 11	+13.0	PN	12	...	...	...
OH 17.7−2.0	18 27 39.8	−14 31 04	+62.0	OH/IR	2	n.o.	~0.6	n.o.
OH 26.5+0.6	18 34 52.5	−05 26 37	+26.5	OH/IR	2	0.80	0.93	0.00
R Aql	19 03 57.7	+08 09 08	+47.0	OH/Mira	9	n.o.	0.42	n.o.
W49	19 07 49.8	+09 01 17	+10.0	MC/H II	3	...	...	...
W51	19 21 27.0	+14 24 30	+55.0	MC/H II	14	...	...	...
Vy 2-2	19 21 59.5	+09 48 00	−61.0	PN	16	...	...	...
IRC +10420	19 24 26.7	+11 15 11	+75.0	OH/SG	2	...	...	...
M1−92	19 34 18.4	+29 26 05	+2.5	BPN	16	...	...	...
V1016 Cyg	19 55 19.8	+39 41 30	0.0	?	17	...	...	...
W75N	20 36 50.0	+42 26 58	+8.0	MC/H II	18	...	...	...
NML Cyg	20 44 33.8	+39 55 57	0.0	OH/SG	2	~0.6	~0.8	~0.9
V1057 Cyg	20 57 06.2	+44 03 46	+1.3	FU Ori	19	...	...	...
V645 Cyg	21 38 10.4	+50 00 35	−43.0	BPN	20	...	...	...
Hb 12	23 23 57.2	+57 54 24	−29.0	PN	12	...	...	...
R Aqr	23 41 14.2	−15 33 42	−28.0	sym?	9	...	...	...
R Cas[d]	23 55 51.9	+51 06 37	+26.0	OH/Mira	10	0.11	0.58	0.89

[a] TYPE ABBREVIATIONS.—AeBe, Herbig Ae-Be object; BPN, bipolar nebula; HH, Herbig-Haro object; FU Ori, FU Orionis–type variable; MC/H II, molecular cloud–H II region; OH/IR, OH/IR star; OH/Mira, OH/Mira variable; OH/SG, OH/supergiant star; sym, symbiotic system; T Tau, T Tauri–type object.

[b] REFERENCES.—(1) Loren, Vanden Bout, and Davis 1973. (2) Bowers, Johnston, and Spencer 1981. (3) Our preferred coordinates. (4) Neugebauer and Leighton 1969. (5) Herbig 1960. (6) Raimond and Eliasson 1969. (7) Strom, Grasdalen, and Strom 1974. (8) Schwartz and Buhl 1975. (9) SAO Catalog. (10) Wynn-Williams, Werner, and Wilson 1974. (11) Kukarkin *et al.* 1969. (12) Perek and Kohoutek 1967. (13) Kwok, Purton, and Keenan 1981. (14) Rickard, Zuckerman, and Palmer 1975. (15) Hardebeck 1972. (16) Davis, Seaquist, and Purton 1979. (17) Purton *et al.* 1982. (18) Haschick *et al.* 1981. (19) Lo and Bechis 1974. (20) Lebofsky *et al.* 1976.

[c] The entry n.o. means no observation of the source on this date.

[d] The phase of R Cas on 1982 May 10 was 0.48.

IV. DISCUSSION

In the following section we summarize the results of the excited-state OH maser searches for objects of the three major categories observed in this study. A brief discussion of ground-state OH emission characteristics and general physical properties is given for each category. More detailed discussions of the structure of Vy 2-2, of pumping models for the excited-state OH, and of radiative transfer of rotationally excited OH follow.

a) Classes of Objects Observed in This Search

i) *Cool Stars of Late M Spectral Type*

Rotationally excited OH masers are weak, if present at all, in this category of objects that includes OH/IR stars, OH/Miras, and OH/supergiants. We searched for the 4.7 and 6.0 GHz main-line and satellite line analogs of the 1.6 GHz ground-state OH transitions in numerous sources, setting upper limits for flux densities usually $\lesssim 10^{-1}$ and in some cases $\lesssim 10^{-2}$ that of observed ground-state lines. In the OH ground rotational

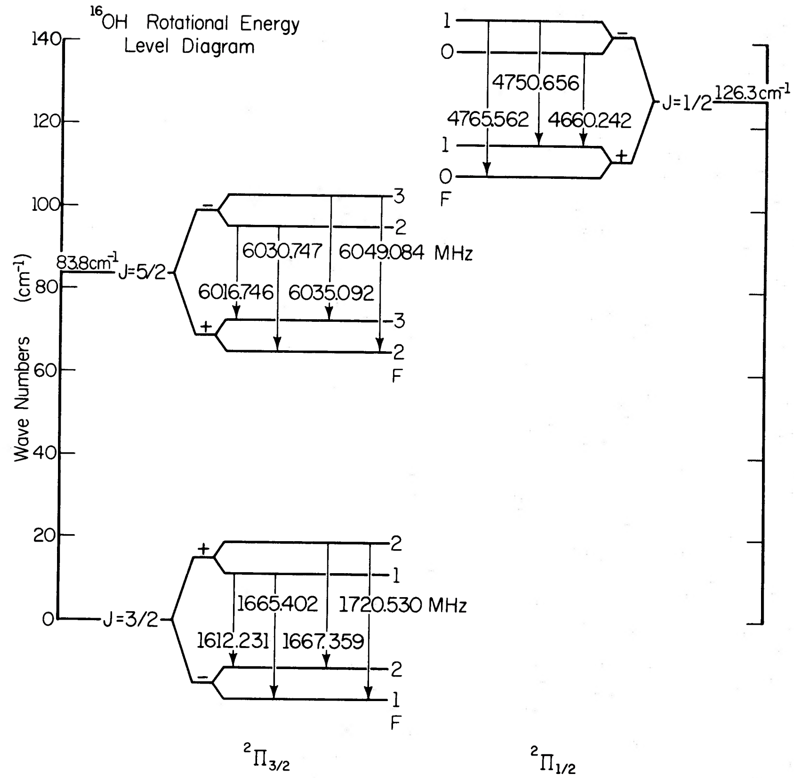

FIG. 1.—The energy level diagram for the first three rotational states of OH. The levels are labeled by rotational quantum number J, lambda doublet partity (+ or −), and hyperfine quantum number F. Transition frequencies are in MHz. The levels studied in this paper are the $^2\Pi_{3/2}$, $J = 5/2$ and $^2\Pi_{1/2}$, $J = 1/2$ excited rotational states.

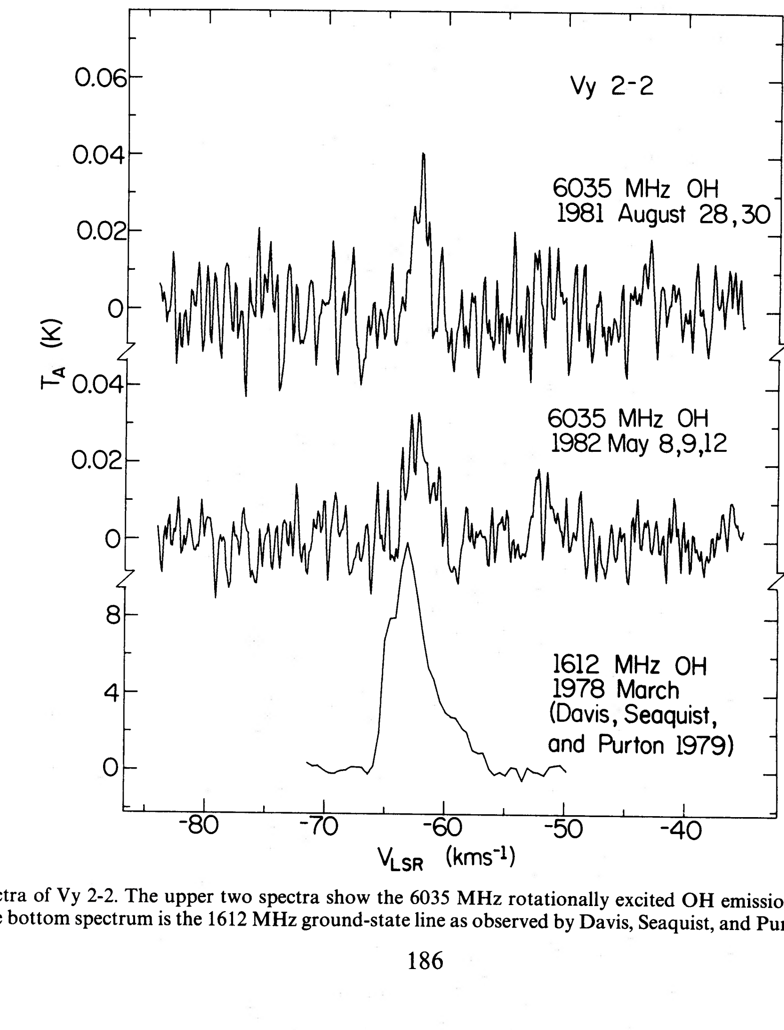

FIG. 2.—The OH maser spectra of Vy 2-2. The upper two spectra show the 6035 MHz rotationally excited OH emission reported in this paper, as observed in 1981 August and 1982 May. The bottom spectrum is the 1612 MHz ground-state line as observed by Davis, Seaquist, and Purton (1979).

1985ApJ...295..183J

TABLE 3

RESULTS OF ROTATIONALLY EXCITED OH OBSERVATIONS

Source	Freq. (MHz)	Pk-Pk Noise (K)	Δv_{ac} (km s^{-1})[a]	V_{range} (km s^{-1})[b]	Date
Lk Hα 198	4750	0.166	0.308	−56, +91	5/82
	4765	0.212	0.307	−56, +91	5/82
	6030	0.114	0.243	−41, +75	5/82
	6035	0.131	0.243	−40, +75	5/82
IRC +10011 ...	4660	0.412	0.079	−28, +47	9/80
		0.349	0.157	−65, +86	8/81
	4750	0.374	0.077	−27, +47	9/80
	4765	0.399	0.077	−27, +49	9/80
	6016	0.231	0.122	−19, +39	4/81
		0.132	0.122	−19, +39	8/81
	6030	0.228	0.121	−19, +39	4/81
	6035	0.202	0.121	−19, +39	4/81
		0.126	0.121	−19, +39	8/81
	6049	0.291	0.121	−19, +39	4/81
OH 127.8−0.0 .	6030	0.329	0.121	−83, −25	4/81
	6035	0.320	0.121	−83, −25	4/81
W3(OH)	4750	0.527	0.077	−81, −7	9/80
	4765	det.	0.077	−81, −7	9/80
	6030	det.	0.121	−72, −15	4/81
		det.	0.121	−72, −14	8/81
		det.	0.121	−72, −14	5/82
	6035	det.	0.121	−72, −15	4/81
		det.	0.121	−72, −14	8/81
		det.	0.121	−72, −15	5/82
IK Tau	6030	0.281	0.121	+5, +63	4/81
	6035	0.288	0.121	+5, +63	4/81
IRC +50137 ...	6030	0.246	0.121	−23, +35	4/81
	6035	0.226	0.121	−23, +35	4/81
HK Ori	6030	0.096	0.243	−40, +71	5/82
	6035	0.099	0.243	−40, +71	5/82
Orion A	4660	det.	0.079	−26, +46	9/80
		det.	0.079	−30, +46	8/81
	4750	0.704	0.077	−24, +45	9/80
	4765	0.633	0.077	−29, +45	9/80
	6030	0.381	0.121	−21, +37	4/81
	6035	0.404	0.121	−21, +37	4/81
M78	6030	0.081	0.243	−51, +60	5/82
	6035	0.076	0.243	−51, +60	5/82
OH 205.1−14.1	6030	0.076	0.243	−52, +60	5/82
	6035	0.066	0.243	−52, +60	5/82
U Ori	6030	0.132	0.121	−67, −14	4/81
	6035	0.132	0.121	−67, −14	4/81
HD 250550	4750	0.142	0.308	−61, +86	5/82
	4765	0.151	0.307	−61, +86	5/82
	6030	0.099	0.243	−46, +70	5/82
	6035	0.118	0.243	−46, +70	5/82
HD 44179	6030	0.078	0.243	−29, +87	5/82
	6035	0.081	0.243	−29, +87	5/82
VY CMa	4660	0.302	0.157	−53, +98	8/81
	4750	0.278	0.154	−52, +97	9/80
	4765	0.342	0.154	−52, +97	9/80
	6016	0.213	0.122	−36, +81	4/81
	6030	0.313	0.121	−36, +81	4/81
		0.149	0.121	−36, +81	8/81
	6035	0.236	0.121	−36, +81	4/81
		0.232	0.121	−36, +81	8/81
OH 231.8+4.2 .	4750	0.343	0.154	−43, +106	9/80
	4765	0.388	0.154	−42, +106	9/80
	6016	0.297	0.122	−27, +90	4/81
	6030	0.355	0.121	−27, +90	4/81
	6035	0.255	0.121	−27, +90	4/81
		0.141	0.121	−27, +90	8/81
AU Gem	4750	0.125	0.154	−30, +43	5/82
	4765	0.116	0.154	−30, +40	5/82
	6030	0.116	0.121	−23, +35	5/82
	6035	0.111	0.121	−23, +35	5/82
R Leo	4660	0.291	0.157	−73, +78	8/81
	4750	0.389	0.077	−35, +39	9/80
		0.180	0.154	−34, +39	8/81
	4765	0.339	0.077	−35, +39	9/80
		0.191	0.154	−34, +39	8/81
	6016	0.245	0.122	−27, +31	4/81
	6030	0.168	0.121	−27, +31	4/81
		0.163	0.121	−27, +31	8/81
	6035	0.206	0.121	−27, +31	4/81
		0.138	0.121	−27, +31	8/81
	6049	0.308	0.121	−27, +31	4/81
W Hya	4660	0.444	0.079	+3, +79	9/80
	4750	0.439	0.077	+4, +78	9/80
	4765	0.377	0.077	+4, +78	9/80
	6016	0.334	0.122	+12, +70	4/81
	6030	0.233	0.121	+12, +70	4/81
		0.172	0.121	+12, +70	8/81
	6035	0.229	0.121	+12, +70	4/81
		0.154	0.121	+12, +70	8/81
	6049	0.324	0.121	+12, +70	4/81
S CrB	6016	0.179	0.122	−27, +31	4/81
	6030	0.260	0.121	−27, +31	4/81
	6035	0.263	0.121	−27, +31	4/81
	6049	0.245	0.121	−27, +31	4/81
WX Ser	4750	0.160	0.154	−29, +44	8/81
	4765	0.155	0.154	−30, +44	8/81
	6016	0.273	0.122	−22, +36	4/81
	6030	0.311	0.121	−22, +36	4/81
	6035	0.337	0.121	−22, +36	4/81
	6049	0.296	0.121	−22, +36	4/81
U Her	6030	0.149	0.121	−42, +16	4/81
	6035	0.118	0.121	−42, +16	4/81
M2−9	6030	0.091	0.243	+26, +142	5/82
	6035	0.083	0.243	+26, +142	5/82
NGC 6334N	6030	det.	0.121	−38, +20	4/81
	6035	det.	0.121	−38, +20	4/81
M3−38	6030	0.093	0.243	−56, +60	5/82
	6035	0.105	0.243	−56, +60	5/82
M1−26	6030	0.115	0.243	−51, +65	5/82
	6035	0.104	0.243	−51, +65	5/82
Sgr B2	4660	det.	0.079	+28, +104	9/80
		det.	0.157	−14, +137	8/81
	4750	det.	0.077	+29, +103	9/80
		det.	0.154	+25, +98	8/81
	4765	det.	0.077	+29, +103	9/80
		det.	0.154	+24, +98	8/81

1985ApJ...295..183J

TABLE 3—*Continued*

Source	Freq. (MHz)	Pk-Pk Noise (K)	Δv_{ac} (km s^{-1})[a]	V_{range} (km s^{-1})[b]	Date
Sgr B2[c] (continued)	6016	0.523	0.122	+32, +90	4/81
	6030	0.419	0.121	+32, +90	4/81
		det.?	0.121	+32, +90	8/81
	6035	det.	0.121	+32, +90	4/81
		det.	0.121	+37, +90	8/81
	6049	0.432	0.121	+32, +90	4/81
VX Sgr	4660	0.469	0.079	−31, +45	9/80
	4750	0.278	0.077	−30, +44	9/80
	6016	0.267	0.122	−22, +36	4/81
	6030	0.186	0.121	−22, +36	4/81
	6035	0.202	0.121	−22, +36	4/81
	6049	0.306	0.121	−22, +36	4/81
SwSt 1	4750	0.175	0.243	−71, +76	5/82
	4765	0.201	0.243	−71. +76	5/82
	6030	0.120	0.243	−56, +60	5/82
	6035	0.126	0.243	−56, +60	5/82
M17	6030	det.	0.121	−6, +51	4/81
	6035	det.	0.121	−6, +51	4/81
		det.	0.121	−6, +51	5/82
IRC −10414	6030	0.290	0.121	−8, +50	4/81
	6035	0.290	0.121	−8, +50	4/81
M3-27	6030	0.101	0.243	−43, +73	5/82
	6035	0.097	0.243	−42, +73	5/82
OH 17.7−2.0	6016	0.283	0.122	+34, +92	4/81
	6030	0.310	0.121	+34, +92	4/81
	6035	0.408	0.121	+34, +92	4/81
	6049	0.385	0.121	+34, +92	4/81
OH 26.5+0.6	4660	0.515	0.079	−11, +65	9/80
		0.293	0.157	−48, +104	8/81
	4750	0.481	0.077	−10, +64	9/80
		0.137	0.154	−9, +65	8/81
	4765	0.553	0.077	−10, +64	9/80
		0.150	0.154	−9, +64	8/81
	6016	0.280	0.122	−2, +56	4/81
	6030	0.218	0.121	−2, +56	4/81
	6035	0.208	0.121	−2, +56	4/81
	6049	0.248	0.121	−1, +56	4/81
R Aql	6016	0.274	0.122	+19, +77	4/81
	6030	0.218	0.121	+19, +77	4/81
	6035	0.230	0.121	+19, +77	4/81
	6049	0.314	0.121	+19, +77	4/81
W49	4750	0.574	0.154	−25, +48	8/81
	4765	det.	0.077	−26, +48	9/80
		det.	0.154	−25, +48	8/81
		det.	0.154	−25, +48	5/82
	6030	0.537	0.121	−18, +40	4/81
		0.684	0.121	−18, +40	8/81
		0.377	0.121	−18, +40	5/82
	6035	det.	0.121	−18, +40	4/81
		det.	0.121	−18, +40	8/81
		det.	0.121	−18, +40	5/82
W51	6030	det.	0.121	+31, +88	5/82
	6035	det.	0.121	+30, +88	5/82
Vy 2-2	4660	0.186	0.157	−97, −22	5/82
	4750	0.133	0.154	−96, −23	5/82
	4765	0.111	0.154	−94, −23	5/82
	6016	0.123	0.122	−89, −31	5/82
	6030	0.081	0.121	−89, −35	8/81
		0.079	0.121	−84, −36	5/82
	6035	det.	0.121	−89, −35	8/81
		det.	0.121	−84, −36	5/82
	6049	0.152	0.121	−88, −30	5/82
IRC +10420	4750	0.226	0.154	+2, +151	8/81
	4765	0.242	0.154	+3, +151	8/81
	6016	0.307	0.122	+18, +135	4/81
		0.141	0.122	+18, +135	8/81
	6030	0.178	0.121	+18, +135	4/81
		0.107	0.121	+18, +135	8/81
	6035	0.156	0.121	+18, +135	4/81
M1-92	4750	0.112	0.154	−68, +79	5/82
	4765	0.142	0.154	−68, +78	5/82
	6030	0.067	0.243	−53, +58	5/82
	6035	0.063	0.243	−53, +58	5/82
V1016 Cyg	6030	0.092	0.243	−56, +60	5/82
	6035	0.113	0.243	−56, +60	5/82
W75N	6030	0.495	0.121	−20, +38	8/81
	6035	det.	0.121	−20, +38	8/81
NML Cyg	4660	0.352	0.079	−37, +39	9/80
		0.281	0.157	−76, +75	8/81
	4750	0.274	0.077	−36, +38	9/80
		0.175	0.154	−37, +36	8/81
	4765	0.373	0.077	−36, +38	9/80
		0.163	0.154	−37, +36	8/81
	6016	0.332	0.122	−57, +60	4/81
	6030	0.305	0.121	−57, +60	4/81
		0.142	0.121	−30, +28	8/81
	6035	0.175	0.121	−57, +60	4/81
		0.168	0.121	−30, +28	8/81
V1057 Cyg	6030	0.154	0.121	−26, +32	8/81
	6035	0.179	0.121	−27, +31	8/81
V645 Cyg	6030	0.110	0.243	−99, +17	5/82
	6035	0.116	0.243	−99, +17	5/82
Hb 12	4750	0.124	0.308	−100, +47	5/82
	4765	0.109	0.307	−100, +47	5/82
	6030	0.085	0.243	−85, +31	5/82
	6035	0.093	0.243	−84, +31	5/82
R Aqr	6030	0.250	0.121	−56, +2	8/81
	6035	0.218	0.121	−56, +2	8/81
R Cas	4660	0.411	0.079	−11, +65	9/80
		0.193	0.157	−48, +103	8/81
	4750	0.444	0.077	−10, +64	9/80
	6030	0.307	0.121	−2, +56	4/81
		0.271	0.121	−2, +56	8/81
	6035	0.287	0.121	−2, +56	4/81
		0.242	0.121	−2, +56	8/81
		0.133	0.121	0, +56	5/82

[a] Autocorrelator channel spacing.
[b] Velocity coverage of the spectrum.
[c] A broad emission pedestal may be present in the Sgr B2 6030 MHz spectrum of 4/81.

TABLE 4

DETECTED LINES OF ROTATIONALLY EXCITED OH

Source	Freq. (MHz)	Date	Peak T_A (K)	RMS Noise (K)	V_{LSR} (km s^{-1})[a,b]	ΔV_{FWHM} (km s^{-1})[c]	V_{range} (km s^{-1})[d]	Notes[e]
W3(OH)	4765	9/80	1.39	0.093	−45.0	0.31	−45.3 − −42.8	
			0.93		−43.3	0.46		
	6030	4/81	7.72	0.067	−42.9	0.73B	−48.5 − −41.8	
		8/81	7.42	0.077	−42.9	0.73B	−48.2 − −41.6	
		5/82	7.44	0.060	−42.8	0.73B	−48.5 − −41.6	
	6035	4/81	29.2	0.064	−43.0	0.73B	−49.0 − −39.1	
		8/81	26.8	0.076	−43.0	0.73B	−49.2 − −40.1	
		5/82	25.6	0.064	−43.0	0.73B	−49.7 − −39.3	
Orion A	4660	9/80	0.22	0.051	+9.8	0.71	+7.9 − +16.1	Hsm.
			0.39		+14.5	0.78		
		8/81	0.19	0.058	+9.8	0.64	+8.7 − +15.8	Hsm.
			0.25		+14.5	0.63		
NGC 6334N ...	6030	4/81	1.31	0.110	−10.4	0.61B	−10.7 − −10.1	
	6035		26.4	0.108	−10.3	0.48B	−11.7 − −6.6	
Sgr B2	4660	9/80	0.18	0.087	+60.0	15.7	+47.4 − +72.0	ped.
		8/81	0.19	0.106	+60.0	20.0	+49.7 − +74.0	ped.
	4750	9/80	0.12	0.040	+57.4	25.3	+44.0 − +72.8	ped.; Hsm.
			0.24		+62.9	0.69		narrow feature
		8/81	0.13	~0.07	+58.3	29.1	+43.6 − +72.7	ped.
	4765	9/80	0.32	0.519	+61.3	0.54	?	Hsm.
		8/81	0.37	0.074	+61.2	0.61	?	possible ped.
	6030	8/81	0.1?	0.065	~+57	~24	+47 − +70	
	6035	4/81	1.40	0.074	+66.6	0.73	+62.2 − +73.1	
			1.60		+72.1	0.85		
		8/81	1.23	0.069	+66.6	0.61B	+62.5 − +72.8	
			1.46		+72.2	0.85B		
M17	6030	4/81	0.46	0.134	+21.5	0.36	+21.2 − +23.1	
			0.44		+22.6	0.36		
	6035	4/81	11.4	0.137	+21.4	0.24	+20.9 − +23.2	
			6.45		+22.5	0.24		
		5/82	11.2	0.167	+21.4	0.36	+21.0 − +23.7	
			6.33		+22.5	0.36		
W49	4765	9/80	0.52	0.111	+8.2	0.23	+8.1 − +8.5	
		8/81	0.41	0.087	+8.2	0.61	+6.5 − +8.6?	
		5/82	0.39	0.056	+8.3	0.31	+8.0 − +8.8	
	6035	4/81	0.55	0.082	+10.3	0.61	+9.9 − +18.4	
			0.43		+13.4	0.85		
			0.26		+16.9	0.61		
			0.37		+18.3	0.61B		
		8/81	0.38	0.098	+10.1	1.09	+9.5 − +18.4	
			0.38		+13.8	0.73		
			0.26		+17.0	0.24		
			0.33		+18.0	0.36		
		5/82	0.38	0.037	+10.4	1.21	+9.9 − +18.8	
			0.38		+13.4	0.85		
			0.30		+17.0	0.24		
			0.23		+18.0	0.48		
W51	6030	5/82	0.91	0.096	+53.6	0.73	+51.8 − +54.0	
	6035	5/82	1.82	0.087	+53.7	0.61	+52.3 − +59.4	
			1.03		+55.1	0.61		
			0.39		+57.1	0.73		
			0.63		+58.5	0.61		
Vy 2-2	6035	8/81	0.041	0.008	−62.3	1.46	−63.7 − −61.4	Hsm.
		5/82	0.033	0.006	−62.4	1.70	−63.8 − −60.4	Hsm.
			0.019?		−52.3	1.58	−53.2 − −50.4	Possible det.
W75N	6035	8/81	1.82	0.081	+6.9	<0.24	+5.8 − +9.8	
			2.30		+8.1	0.61		
			0.58		+9.6	0.73		

[a] Because of a slight inaccuracy in the procedure which set the center velocity of the Model IV autocorrelator during its early operation, the velocity scales for the 9/80 and 4/81 data were subject to errors of ~2–5 channels. We believe that the velocities listed here have been largely corrected for this problem, but errors ≤0.3 km s^{-1} may still exist.

[b] The LSR velocities denote the velocity of peak emission except in the case of pedestal emission (Sgr B2) where it denotes the center of the pedestal.

[c] A notation of "B" on the velocity widths indicates that the line is composed of a blend of semiresolved features.

[d] V_{range} indicates the velocity range of the emission complex.

[e] A notation of "Hsm." indicates that the peak emission and rms noise were taken from a Hanning smoothed spectrum; "ped." indicates that an emission pedestal was present.

state, OH/IR stars and OH/supergiants typically emit most strongly in the 1612 MHz satellite line although weaker 1665 or 1667 MHz main-line emission is usually present. OH/Miras often emit only in the OH main lines. Using models developed by Goldreich and Scoville (1976) and Elitzur, Goldreich, and Scoville (1976, hereafter EGS), typical physical parameters for circumstellar envelopes at a radius of 3×10^{16} cm are $N_{OH} \approx 10^{16}$ cm^{-2}, $n_{H_2} \approx 10^4$ cm^{-3}, $T_k \lesssim 100$ K, with $T_{dust} \gtrsim T_k$. EGS found that for a standard model with parameters similar to those just listed, the 1612 MHz maser was quenched by collisions for $n_H = n_{H_2} \gtrsim 4 \times 10^5$ cm^{-3}.

ii) *Circumstellar Objects with Hot Central Stars*

The objects in this category are of two different types, compact planetary nebulae and young objects such as Herbig-Haro and Herbig Ae-Be stars. One compact planetary nebula, Vy 2-2 was detected. The emission was observed at two epochs, 9 months apart; within the noise, there is no evidence for variability between the two observations. The ratio of 6035 MHz to 1612 MHz flux in this source is 0.026 (photon flux ratio $\phi_{6035}/\phi_{1612} = 6.9 \times 10^{-3}$).

The negative results for the other compact planetaries might be caused by inadequate sensitivity, inappropriate chemistry (carbon-rich rather than oxygen-rich), or a dissipated red giant circumstellar envelope. Presumably, the phase of red giant mass loss has ended in these objects. Within $\sim 10^4$ yr, the density of the gas and the density and temperature of the dust will become inadequate to support OH maser emission, if the gas is flowing out at a rate of a few km s^{-1}. Hence, this phase of evolution is brief. The young objects were included on the chance that their physical environment might resemble that of Vy 2-2, despite the difference in evolutionary stages.

iii) *Compact* H II *Regions Associated with Star Formation*

Rotationally excited OH masers in the $^2\Pi_{3/2}$, $J = 5/2$ and $^2\Pi_{1/2}$, $J = 1/2$ levels are commonly found in these regions. The 1665 and 1667 MHz main lines are the dominant ground-state OH masers in these regions; the 1612 MHz and 1720 MHz lines are usually much weaker, although some strong masers at these frequencies do exist (Guilloteau 1982). In general, however, main-line masers predominate among lambda doublets in the $^2\Pi_{3/2}$ ladder. This is in contrast with the $^2\Pi_{1/2}$, $J = 1/2$ lambda doublet in which 4765 MHz emission—the analog of the ground-state 1720 MHz line— is strongest.

Despite the general association of ground- and excited-state OH masers in these regions, the velocity of peak emission is typically different for different rotational states (e.g., Winnberg, Walmsley, and Churchwell 1978). This indicates that the strongest ground- and excited-state masers usually exist in different volumes of gas. Physical conditions in these regions are typically $T_k = 100$–200 K, $n_{H_2} \approx 10^7$ cm^{-3}, and $N_{OH} \approx 10^{17}$ cm^{-2} (Guilloteau 1982). More details about these objects are given by Guilloteau *et al.* (1984) and references therein.

b) *Vy 2-2: Morphology and Maser Excitation*

To date, most of the information on the structure of the neutral envelope about Vy 2-2 has been provided by the 1612 MHz OH maser. DSP proposed a source morphology similar to OH/IR stars from the line profile shape of the 1612 MHz emission (Fig. 2) which resembles the blueshifted half of the double-peaked OH maser emission pattern of OH/IR stars. In the idealized OH/IR star model (e.g., EGS; Kwok 1976; Reid *et al.* 1977), the two emission peaks of the OH/IR stars arise from masers situated along the line of sight through the star with the low-velocity, or blueshifted, maser residing at the near side of the radially expanding envelope and the high-velocity, redshifted maser residing at the far side. The weak emission between the main peaks appears in spatial maps as concentric rings centered on the line of sight through the star (Booth *et al.* 1981). DSP suggested that the redshifted emission was absent in Vy 2-2 because the intervening ionized region, which is optically thick up to a frequency of ~ 15 GHz (Seaquist and Davis 1983), absorbed it. Alternatively, Kwok (1981) suggested that the far component was missing because, geometrically, the gas is unable to amplify the 18 cm continuum radiation of the nebula along the observer's line of sight, whereas the front side can . The latter explanation is possible only if the 1612 MHz maser is unsaturated, however (Elitzur 1982).

Recently, spatial maps of the ionized region and the 1612 MHz OH maser using the Very Large Array have been made by Seaquist and Davis (1983). At 15 GHz, the ionized nebula was resolved as a thin shell, $\sim 0\farcs5$ in outer diameter and $\sim 0\farcs2$ in inner diameter. The peak OH maser emission is projected on the outer periphery of the 15 GHz continuum emission region; the weaker, high-velocity 1612 MHz wing originates from a string of positions directed outward from the ionized region and the postion of peak OH emission. Thus, the 1612 MHz OH maser emission of Vy 2-2 does not conform to the idealized OH/IR star model. This is not unusual for OH/IR stars and may indicate only that the envelope is clumpy rather than homogeneous. However, Seaquist and Davis (1983) suggested that the 1612 MHz maser emission might be in the shocked, density-enhanced zone at the interface of the neutral and ionized regions. In this case, the OH maser emission distribution would probably bear no resemblance to that of OH/IR stars. Since physical conditions will vary greatly, determination of whether the masers are located in this region or far out in the circumstellar envelope as in the OH/IR star model may indicate whether they are radiatively or collisionally pumped.

The LSR velocity of the Vy 2-2 nebula as determined from optical spectra is -53.9 ± 3.9 km s^{-1} (Schneider *et al.* 1983). Recently, Knapp and Morris (1984) have reported a tentative detection of CO emission from Vy 2-2 at a center velocity of approximately -45 km s^{-1} and extending from about -56 to about -32 km s^{-1}. The optical and CO velocities are somewhat inconsistent with each other, although either could be consistent with an OH/IR star expanding envelope model. The CO detection is too marginal to provide firm conclusions at this time, however.

The 6035 MHz OH maser emission reported here may help clarify the morphology of Vy 2-2. The -62 km s^{-1} feature at 6035 MHz occurs at about the same velocity as the peak 1612 MHz emission (Fig. 2). In addition, there is in the 1982 May 6035 MHz spectrum a possible line at -52.3 km s^{-1}. This feature is at the 3 σ level and will have to be confirmed. If real, it could be interpreted in terms of the OH/IR star model as the missing velocity component from the far side of the nebula. The previously mentioned argument that 1612 MHz emission from the far side of the nebula would be absorbed would generally hold for 6035 MHz emission as well. If we assume that $\tau(15 \text{ GHz}) = 1$ and $T_e = 10^4$ K, then by scaling laws (Spitzer 1978, p. 59), $\tau(6 \text{ GHz}) = 7$ whereas $\tau(1.6 \text{ GHz}) = 110$. Thus, even though the 6035 MHz optical depth is substantial, masers at the far side of the nebula but at its periphery might not be entirely absorbed by the intervening ionized material.

c) *Pumping and Radiative Transfer of Rotationally Excited* OH *Masers*

The characteristics of the Vy 2-2 masers are anomalous: a satellite line (1612 MHz) is strongest in the ground state, while a main line (6035 MHz) is strongest in the first excited state. As summarized above, this is atypical of both young H II regions and OH/IR stars, where rotationally excited OH lines may not exist at all. An explanation of the Vy 2-2 characteristics that is consistent with the negative results for the other evolved stars is the primary challenge of any model of circumstellar rotationally excited OH masers. The feasibilities of various models are discussed below.

i) *Radiative Pumps*

Noting that Vy 2-2 is a copious emitter of infrared radiation, DSP suggested that the far-IR pumping model of EGS might explain the 1612 MHz OH maser in the source. The EGS model has been successful in explaining 1612 MHz masers from cool, evolved stars. In its simplest form, this model is not expected to produce *main-line* OH masers, however. Indeed, in their model calculations EGS found no inversions in the $^2\Pi_{3/2}$, $J = 5/2$ levels responsible for the 6035 MHz emission. Furthermore, the population per degenerate sublevel in the $^2\Pi_{3/2}$, $J = 5/2$ states was $\sim 10^{-3}$ smaller than in the ground state, although the input parameters used may be dissimilar to those obtaining in Vy 2-2. Nevertheless, variations of this model which take into account more subtle physical effects may explain the ground-state main lines. Such models may be relevant to rotationally excited main lines, as well.

In Figure 3, we display an OH energy level diagram showing the simplified path of the 35 μm pump, and the allowed transitions between *rotational* levels. The Einstein *A*-coefficients as obtained from Brown *et al.* (1982) are given for each transition. In the absence of photon trapping effects, the flow path will proceed according to the *A*-coefficients. Thus, following the 35 μm pump transition from the ground $^2\Pi_{3/2}$, $J = 3/2$ state to the $^2\Pi_{1/2}$, $J = 5/2$ state, the radical will decay down the $^2\Pi_{1/2}$ ladder via infrared rotational transitions until it reaches the $^2\Pi_{1/2}$, $J = 1/2$ state. From there, the only remaining allowed transition is to the $^2\Pi_{3/2}$, $J = 3/2$ ground state. Simple dipole selection rules together with photon trapping effects in the final IR transition produce the inversion in the 1612 MHz levels.

Since the two halves of the lambda doublets are symmetric to dipole selection rules, an inversion of the OH main lines does not result from a simple cascade through rotational levels. Elitzur (1978) noted that the energy separation of the two halves of the lambda doublets increases through the $^2\Pi_{1/2}$, $J = 5/2$ state. If the intensity of the infrared pumping radiation also increases with frequency—as it will for hot, optically thin dust—the upper halves of the lambda doublets will be preferentially populated and main-line inversion will result. Bujarrabal *et al.* (1980) found that asymmetries in the Einstein *A*-coefficients of OH for infrared transitions led to stronger inversions when pumping is by a frequency-dependent spectrum as described above.

This mechanism could well explain the 6035 MHz maser of Vy 2-2. However, the $^2\Pi_{3/2}$, $J = 5/2$ levels are efficiently involved in the pump cycle described above only when the $^2\Pi_{1/2}$, $J = 3/2 \rightarrow 1/2$ *and* the $^2\Pi_{1/2}$, $J = 3/2 \rightarrow {}^2\Pi_{3/2}$, $J = 3/2$ transitions are at least partially saturated. Because of the presumed large abundance in the ground state, rotational transitions connecting the ground state are probably optically thick in any case, so the $^2\Pi_{1/2}$, $J = 3/2 \rightarrow 1/2$ transition is the most critical. This transition will achieve a peak optical depth of unity (see the Appendix) under physical conditions similar to those giving rise to 1612 MHz OH maser emission in the model of EGS, e.g., $T_{ex} = 50$ K, $n_l(\text{OH}) = 5 \times 10^{-4}$ cm^{-3}, $L = 10^{16}$ cm, and $\Delta v = 1$ km s^{-1}. Thus, no extraordinary conditions are required for the $^2\Pi_{3/2}$, $J = 5/2$ levels to become part of the far-IR pump cycle. Such a model is worthy of further, more detailed calculations.

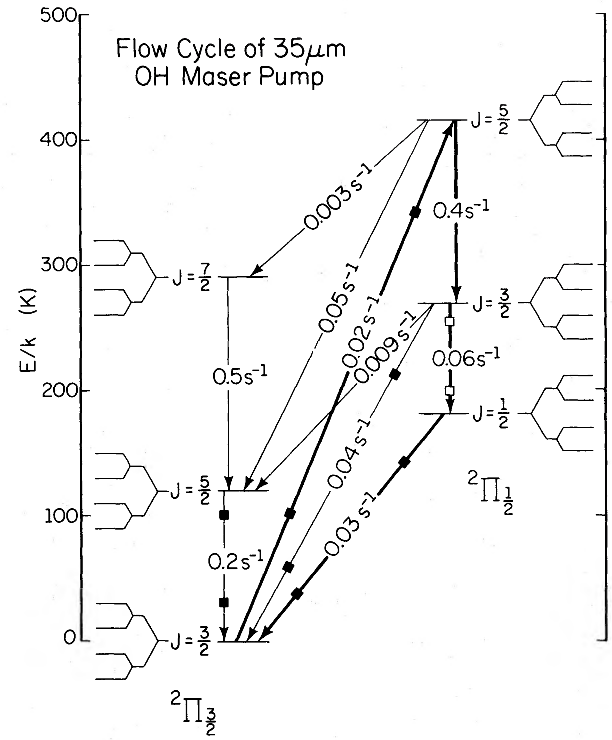

FIG. 3.—The flow cycle of the 35 μm radiative pump of the OH maser. The bold lines indicate the transitions involved in the inversion of the ground-state 1612 MHz maser as proposed by Elitzur, Goldreich, and Scoville (1976). (The lambda doubling and hyperfine splittings are ignored in this qualitative description). The Einstein spontaneous emission coefficients are given for the most probable transition connecting two lambda doublets (data from Brown *et al.* 1982). Rotational transitions connecting the ground-state lambda doublet are presumed to be optically thick and are so designated by the filled squares in the figure. Additionally, if the $^2\Pi_{3/2}$, $J = 5/2$ levels are to participate in the pump cycle, then the transitions connecting the $^2\Pi_{1/2}$, $J = 3/2$ and 1/2 levels (marked by an open square) must be at least partially optically thick.

ii) *Collisional Pump Models*

Collisional pumping has been advocated by Flower and Guilloteau (1982) as a likely excitation mechanism for excited-state OH masers near H II regions. This model uses recently calculated cross sections for para-H_2–OH collisions and requires that the gas kinetic temperature T_k exceed the dust temperature T_d. High maser brightness temperatures are produced for physical conditions typical of H II region/molecular cloud interfaces. A typical gas density in these regions is $n_{H_2} \approx 10^7$ cm^{-3}, at least 10^2 larger than in the OH maser regions of cool IR stars. As a result, collisional pumping is probably insignificant in OH/IR stars and OH/Miras for either the ground or excited rotational states of OH.

The possibility that a collisional pump could explain the Vy 2-2 6035 MHz OH maser must be given serious consideration. The Vy 2-2 envelope is apparently an H II region expanding into a neutral molecular cloud, and physical conditions could be similar to those in interstellar OH/H II regions. Specifically, a shocked, high-temperature and high-density zone with characteristics comparable to those of OH/H II regions could exist near the interface of the ionized and neutral regions of Vy 2-2. Moreover, the kinetic temperature throughout the envelope is likely to be higher than in an OH/IR star because of the high excitation of the central star and nebula. More extensive modeling of the neutral and ionized nebulae and observations of other molecular species such as CO should eventually lead to accurate physical parameters for Vy 2-2 and an assessment of collisional pumping of OH.

iii) *Radiative Transfer of Rotationally Excited* OH *Maser Emission*

Most astrophysical masers are believed to exist in long, tubelike columns of gas (Elitzur 1982). The brightness temperature of a cylindrical maser may be written as (see the Appendix)

$$T_B = \frac{7}{12}\frac{h^2c^3}{8\pi k^2}\frac{L^2}{r^2}\frac{\Gamma f N_{OH}}{\nu^2 \Delta v}\left(-\frac{\nu}{T_0}\right), \tag{1}$$

where Γ is the damping constant (inverse lifetime) of the inversion states; L is the length of the maser cylinder and r is its radius; f is the fraction of OH molecules in the lower level of the transition; N_{OH} is the total OH column density; Δv is the line width; and T_0 is the unsaturated excitation temperature. The brightness temperature is related to the observed flux density S by $T_B = \lambda^2 S/2k\Omega_s$, so long as the source solid angle Ω_s is small compared to the antenna main beam solid angle.

From the observed flux density of the 6035 MHz maser of Vy 2-2, we would like to determine such quantities as T_0 and fN_{OH}. Similarly, for the nondetections in other sources, we would like to place limiting values on these quantities. Unfortunately, few of the other required parameters in equation (1) are well determined, so we must seek ways to eliminate some parameters. Since size parameters such as L/r and Ω_s are set by the physical scale of the circumstellar envelope and can be presumed to be comparable for 6035 MHz and 1612 MHz OH masers, a fruitful approach is to deal in ratios of 6035 MHz to 1612 MHz flux densities. Interpreted in the terms of equation (1), these ratios become

$$\frac{S_{6035}}{S_{1612}} \approx \frac{(\Gamma f \nu/T_0)_{6035}}{(\Gamma f \nu/T_0)_{1612}}, \tag{2}$$

where Ω_s and L/r are assumed equal for the two transitions.

The detected ground- and excited-state OH lines in Vy 2-2 are in the ratio $S_{6035}/S_{1612} = 0.026$. The strength of the 6035 MHz line here may be explained by a slightly larger population in the maser levels. In thermal equilibrium at $T = 50$ K, $f_{6035}/f_{1612} = 0.13$. Because of the fast IR radiative transitions out of the $^2\Pi_{3/2}$, $J = 5/2$ states, the thermal equilibrium population is probably an upper limit to the actual population (at that temperature). High fractional populations in the 6035 MHz levels in Vy 2-2 would be expected if the maser resides near the interface of the H II region and molecular cloud. The fractional population ratio might then be bounded by the thermal equilibrium value and the value typical of OH/IR stars (see, for example, Table 2 of EGS), i.e., $0.13 \leq f_{6035}/f_{1612} \leq 0.001$. This range is quite consistent with the Vy 2-2 flux density ratio of 0.026 if ν/T_0 and Γ are similar for the two masers.

For the negative results of OH/IR stars, the flux density ratio $S_{6035}/S_{1612} \leq 1.8 \times 10^{-3}$ for OH 26.5 + 0.6, $\leq 1.2 \times 10^{-3}$ for NML Cyg, and ≤ 0.013 for IRC +10011. Thus, regardless of the values of Γ and T_0, the difference in population between the 1612 and 6035 MHz maser states is sufficient to explain the negative results at 6035 MHz. The possibility that the relative inversion ν/T_0 or the lifetime Γ is greatly stronger at 6035 MHz than at 1612 MHz is also precluded.

V. CONCLUSIONS

The observations and analysis of this paper suggest the following conclusions regarding rotationally excited OH in circumstellar envelopes. For cool objects such as OH/Miras and OH/IR stars, the lack of rotationally excited OH emission results primarily from the small population in those levels; whether the levels are inverted or not is generally academic. The possibility that episodic flares of excited-state OH emission occur in some of these stars cannot be ruled out, however.

The existence of excited-state OH emission in Vy 2-2 can probably be attributed to the high excitation of that source. Several possibilities for the pump mechanisms and locations of the 1612 MHz masers can be enumerated:

1. The two masers are not spatially associated; the 1612 MHz maser exists far out in the remnant circumstellar envelope and is pumped by 35 μm radiation but the 6035 MHz maser exists in a higher density region near the ionized nebula and is pumped by collisions. This model is the easiest to explain in terms of other known astrophysical masers and existing pumping theories.

2. The two masers are spatially associated in the outer circumstellar envelope and both are radiatively pumped, the 1612 MHz maser by the 35 μm mechanism of EGS and the 6035 MHz maser perhaps by mechanisms similar to those proposed by Elitzur (1978) and Bujarrabal *et al.* (1980) for the ground-state main lines.

3. The two masers are spatially associated but are both in a density-enhanced zone near the ionized nebula. Hybrid physical conditions intermediate between those of OH/IR stars and interstellar OH/H II regions could be produced by a shock front advancing into a medium whose density is probably decreasing as r^{-2}. The 1612 and 6035 MHz masers might be pumped by radiation, collisions, or a combination.

The major challenge for any model of these masers is to explain the observed combination of maser transitions, which is very unusual. A strong possibility exists that the physical conditions and the OH masers in Vy 2-2 are unique. The information provided by the masers will undoubtedly play an important role in the eventual explanation of the source.

Further work on the Vy 2-2 OH masers is needed. Among observations, the confirmation of the possible high-velocity 6035 MHz line is important. In addition, interferometer maps showing the relative positioning of 1612 and 6035 MHz maser features are essential. Theoretical work needed includes detailed modeling of the density and temperature profiles of the source and of the pumping and radiative transport of the OH masers.

The authors thank the operators and staff of the NRAO 140 foot telescope for their cooperation during this project. We have also benefited from discussions with Drs. M. Elitzur, S. Guilloteau, and J. B. Kaler. In addition, we thank Dr. L. E. Davis for useful communications and J. A. Mattei of the AAVSO for supplying phase information for long-period variables. Parts of this work were developed for the Ph.D.

dissertation of P. R. J. The use of facilities at the Max-Planck-Institut für Radioastronomie and the National Radio Astronomy Observatory during the completion of this project is greatly appreciated. This work was partially supported by NSF grants 79-07830 and 82-17547, and the University of Illinois Research Board.

APPENDIX

I. THE OPTICAL DEPTH OF OH INFRARED TRANSITIONS

The optical depth τ_ν of a transition is given in terms of the level degeneracies g_i, the Einstein A-coefficient A_{ul}, the column density of the lower level N_l, the transition wavelength λ_0, and the excitation temperature $T_{\rm ex}$ by

$$\int_0^\infty \tau_\nu \, dv = \frac{g_u A_{ul} N_l \lambda_0{}^2}{8\pi g_l} (1 - e^{-hc/\lambda_0 k T_{\rm ex}}) . \tag{A1}$$

Assuming a Gaussian line shape, the ${}^2\Pi_{1/2}$, $J = 3/2$, $F = 2^+ \rightarrow {}^2\Pi_{1/2}$, $J = 1/2$, $F = 1^-$ transition will achieve peak optical depth of unity at a lower level number density of

$$[n_l]_{\tau=1} = 5.7 \times 10^{-4} \left(\frac{10^{16}\ \mathrm{cm}}{L}\right)\left(\frac{\Delta v}{\mathrm{km\ s^{-1}}}\right)\left[1 - \exp\left(\frac{-88.2}{T_{\rm ex}}\right)\right]^{-1} \mathrm{cm}^{-3} , \tag{A2}$$

where a Gaussian line shape of FWHM Δv is assumed, and where L is the path length. For $L = 10^{16}$ cm, $\Delta v = 1$ km s^{-1}, and $T_{\rm ex} = 50$ K, $[n_l]_{\tau=1} = 5 \times 10^{-4}$ cm^{-3}.

II. THE BRIGHTNESS TEMPERATURE OF A CYLINDRICAL MASER

Working from a theory developed by Goldreich and Keeley (1972), Guilloteau, Lucas, and Omont (1981) have given a useful expression for the brightness temperature of a cylindrical maser that may be written as

$$T_B = \frac{7}{12} \frac{hc^3}{8\pi k} \frac{L^3}{r^2} \frac{\Delta n_0 \Gamma}{\nu^2 \Delta v} . \tag{A3}$$

Here, L is the length of the maser cylinder, and r is its radius; Δn_0 is the unsaturated inversion density of molecules in the velocity interval Δv; and Γ is the damping constant of the inversion states. The unsaturated inversion density Δn_0 is related to the unsaturated excitation temperature T_0 by the Boltzmann equation:

$$\Delta n_0 \equiv g_l \left(\frac{n_{u_0}}{g_u} - \frac{n_{l_0}}{g_l}\right) = n_{l_0}(e^{-h\nu/kT_0} - 1) \approx -n_{l_0} \frac{h\nu}{kT_0} , \tag{A4}$$

where n_{u_0} and n_{l_0} are the unsaturated populations of the upper and lower states, respectively, and where the last approximation is valid for weak inversions at maser frequencies important here. Writing the lower level unsaturated population as a fraction of the total OH column density, $n_{l_0} = f n_{\rm OH} = f n_{\rm OH}/L$, where $N_{\rm OH}$ is the OH column density, one obtains the maser brightness temperature expression given in equation (1) of the text.

REFERENCES

Baars, J. W. M., Genzel, R., Pauliny-Toth, I. I. K., and Witzel, A. 1977, *Astr. Ap.*, **61**, 99.
Baudry, A. 1974, *Astr. Ap.*, **32**, 191.
Booth, R. S., Kus, A. J., Norris, R. P., and Porter, N. D. 1981, *Nature*, **290**, 382.
Bowers, P. F., Johnston, K. J., and Spencer, J. H. 1981, *Nature*, **291**, 382.
Brown, J. M., Schubert, J. E., Evenson, K. M., and Radford, H. E. 1982, *Ap. J.*, **258**, 899.
Bujarrabal, V., Guibert, J., Nguyen-Q-Rieu, and Omont, A. 1980, *Astr. Ap.*, **84**, 311.
Claussen, M. J., and Fix, J. D. 1981, *Ap. J. (Letters)*, **250**, L77.
Davis, L. E., Seaquist, E. R., and Purton, C. R. 1979, *Ap. J.*, **230**, 434 (DSP).
Elitzur, M. 1978, *Astr. Ap.*, **62**, 305.
———. 1982, *Rev. Mod. Phys.*, **54**, 1225.
Elitzur, M., Goldreich, P., and Scoville, N. 1976, *Ap. J.*, **205**, 384 (EGS).
Flower, D. R., and Guilloteau, S. 1982, *Astr. Ap.*, **114**, 238.
Goldreich, P., and Keeley, D. A. 1972, *Ap. J.*, **174**, 517.
Goldreich, P., and Scoville, N. 1976, *Ap. J.*, **205**, 144.
Guilloteau, S. 1982, *Astr. Ap.*, **116**, 101.
Guilloteau, S., Baudry, A., Walmsley, C. M., Wilson, T. L., and Winnberg, A. 1984, *Astr. Ap.*, **131**, 45.
Guilloteau, S., Lucas, R., and Omont, A. 1981, *Astr. Ap.*, **97**, 347.
Hardebeck, E. G. 1972, *Ap. J.*, **172**, 583.
Haschick, A. D., Reid, M. J., Burke, B. F., Moran, J. M., and Miller, G. 1981, *Ap. J.*, **244**, 76.
Herbig, G. 1960, *Ap. J. Suppl.*, **4**, 337.
Herman, J. 1983, Ph.D. thesis, Leiden University.
Jewell, P. R., Webber, J. C., and Snyder, L. E. 1980, *Ap. J. (Letters)*, **242**, L29.
Kaler, J. B. 1976, *Ap. J. Suppl.*, **31**, 517.
Knapp, G. R., and Morris, M. 1984, preprint.
Kukarkin B. V., *et al.* 1969, *General Catalogue of Variable Stars* (3d ed.; Moscow: Astronomical Council of the Academy of Sciences in the U.S.S.R.).
Kwok, S. 1976, *J.R.A.S. Canada*, **70**, 49.
———. 1981, in *Physical Processes in Red Giants*, ed. I. Iben, Jr., and A. Renzini (Dordrecht: Reidel), p. 421.
Kwok, S., Purton, C. R., and Keenan, D. W. 1981, *Ap. J.*, **250**, 232.
Lebofsky, M. J., Kleinmann, S. G., Rieke, G. H., and Low, F. J. 1976, *Ap. J. (Letters)*, **206**, L157.
Lo, K. Y., and Bechis, K. P. 1974, *Ap. J. (Letters)*, **190**, L125.
Loren, R. B., Vanden Bout, P. A., and Davis, J. H. 1973, *Ap. J. (Letters)*, **185**, L67.
Marsh, K. A. 1975, *Ap. J.*, **201**, 190.
Meerts, W. L., and Dymanus, A. 1975, *Canadian J. Phys.*, **53**, 2123.
Neugebauer, G., and Leighton, R. B. 1969, *Two-Micron Sky Survey, NASA SP-3047*.
Perek, L., and Kohoutek, L. 1967, *Catalogue of Galactic Planetary Nebulae* (Prague: Academia Publishing House of the Czechoslovak Academy of Sciences).
Purton, C. R., Feldman, P. A., Marsh, K. A., Allen, D. A., and Wright, A. E. 1982, *M.N.R.A.S.*, **198**, 321.
Radford, H. E. 1968, *Rev. Sci. Instr.*, **39**, 1687.
Raimond, E., and Eliasson, B. 1969, *Ap. J.*, **155**, 817.
Reid, M. J., Muhleman, D. O., Moran, J. M., Johnston, K. J., and Schwartz, P. R. 1977, *Ap. J.*, **214**, 60.
Rickard, L. J., Zuckerman, B., and Palmer, P. 1975, *Ap. J.*, **200**, 6.
Schneider, S. E., Terzian, Y., Purgathofer, A., and Perinotto, M. 1983, *Ap. J. Suppl.*, **52**, 399.
Schwartz, P. R., and Buhl, D. 1975, *Ap. J. (Letters)*, **201**, L27.
Seaquist, E. R., and Davis, L. E. 1983, *Ap. J.*, **274**, 659.

Spitzer, L., Jr. 1978, *Physical Processes in the Interstellar Medium* (New York: John Wiley).
Strom, S. E., Grasdalen, G. J., and Strom, K. M. 1974, *Ap. J.*, **191**, 111.
Thacker, D. L., Wilson, W. J., and Barrett, A. H. 1970, *Ap. J. (Letters)*, **161**, L191.
Winnberg, A., Walmsley, C. M., and Churchwell, E. 1978, *Astr. Ap.*, **66**, 431.
Wynn-Williams, C. G., Werner, M. W., and Wilson, W. J. 1974, *Ap. J.*, **187**, 41.
Zuckerman, B., Yen, J. L., Gottlieb, C. A., and Palmer, P. 1972, *Ap. J.*, **177**, 59.

PHILIP R. JEWELL: National Radio Astronomy Observatory, 949 North Cherry Avenue, Campus Building 65, Tucson, AZ 85721-0655

MARK S. SCHENEWERK and LEWIS E. SNYDER: Department of Astronomy, University of Illinois, 341 Astronomy Building, 1011 West Springfield Avenue, Urbana, IL 61801-3000